

Manuscript Details

Manuscript number	ECSS_2019_157_R3
Title	Hydrodynamic forcing and sand permeability influence the distribution of anthropogenic microparticles in beach sediment.
Article type	Research Paper

Abstract

The distribution of anthropogenic microparticles (Mps), such as plastic and natural fibres used in textiles, in beach sediments was studied in a human-influenced pocket beach in Liguria (NW Mediterranean Sea). Information on environmental parameters such as rainfall, hydrodynamism and sediment texture was collected at the same time as the sediment samples. The Mps (416 ± 202 Mps kg⁻¹ on average) were mainly fibres (57-100%), while fragments and spheres showed irregular abundances linked to the draining action of waves on the beach. Uni- and multivariate statistical analyses highlighted that the different spatial and seasonal distribution of fibres primarily depended on the action of the waves that force seawater into the sand, rather than on sedimentation following depositional processes. Wave height and direction had a role in fibre distribution in the sand, as well as sediment permeability and sorting. The occurrence of short-term and spatially-localised hydrodynamic events such as rip currents were observed to influence the abundance of fibres, overlapping the seasonal sequences of beach accretion and erosion that is typical of the area and increasing fibre abundance by transporting those accumulated in the sediments of the submerged beach during winter.

Keywords	anthropogenic microparticles; beach sediment; hydrodynamism; sediment texture; NW Mediterranean.
Taxonomy	Beach Process, Litter, Pollution Impact on Marine Environment
Corresponding Author	Cristina Mistic
Corresponding Author's Institution	Dipartimento di Scienze della Terra, dell'Ambiente e della Vita - University of Genova
Order of Authors	Cristina Mistic, Anabella Covazzi Harriague, Marco Ferrari
Suggested reviewers	Umberto Simeoni, Gerd Liebezeit, Anna Sanchez-Vidal, Andreja Palatinus

Submission Files Included in this PDF

File Name [File Type]

Cover letter.docx [Cover Letter]
Response to reviewer.docx [Response to Reviewers]
Highlights.docx [Highlights]
Mistic et al text third revision.docx [Manuscript File]
Figure 1.tif [Figure]
Figure 2.tif [Figure]
Figure 3.tif [Figure]
Figure 4.tif [Figure]
Figure 5.tif [Figure]
Figure 6.tif [Figure]
Figure 7.tif [Figure]
tables third revision.docx [Table]
Mistic et al - declaration-of-competing-interests.docx [Conflict of Interest]

To view all the submission files, including those not included in the PDF, click on the manuscript title on your EVISE Homepage, then click 'Download zip file'.



UNIVERSITA' DEGLI STUDI DI GENOVA
Dipartimento di Scienze della Terra dell'Ambiente e della Vita (DiSTAV)

Corso Europa, 26 - 16132 GENOVA
C.F.: 00754150100
Fax 010.3538147 - 010 352 169

Genova, 24 September 2019

Dear Editor of Estuarine, Coastal and Shelf Science,

We submit the third revised version of the manuscript "Hydrodynamic forcing and sand permeability influence the distribution of anthropogenic microparticles in beach sediment" by C. Misic, A. Covazzi Harriague and M. Ferrari.

Thank you for your attention and do not hesitate to contact me at the address below for any further requirement.

Looking forward to hearing from you, I remain

Sincerely yours

Cristina Misic

Dr. Cristina Misic

Dipartimento di Scienze della Terra, dell'Ambiente e della Vita,

University of Genova

C.so Europa 26, 16132 Genova - Italy

Phone: 0039 01035338224

e-mail: misic@dipteris.unige.it

Response (in bold) to Reviewer 3

This is an interesting attempt to explain the distribution of microplastic particles in a wave-stirred beach. The English needs a final editing: for instance
-sea calm condition should be calm sea condition
- Hydrodynamism is not in the English online dictionary nor in Thesaurus. Try: 'hydrodynamic nature' etc.

The text has been subjected to a final editing by a native English speaker. The text of the first revision was processed by a certified English proofreading service before (the certificate was attached to the first revised manuscript). “Hydrodynamism” was changed with “hydrodynamic characteristics”. “Sea calm condition” was changed with “calm-sea condition”.

I would personally like to see more thinking and hopefully an additional interpretation about Figure 7. Indeed the January data are the odd points that do not fit in the general pattern. What happened in January (what additional processes occurred?)? With so much scatter in Figure 7 (if the January data are included), hardly any explanation is possible to explain Figure 7, even if statistics give you a 0.5 coefficient of fit - but visually that seems just a coincidence!) and the bottom half of the abstract and much of the highlights are not justified from looking at Figure 7. The data could possibly be explained if the January data were excluded provided other processes dominated in January and are explained or at least suggested? Can you do some statistics on that to better explain the hydrodynamics of the microplastic particles in different seasons?

In the text (lines 804-811 in Results section, lines 899-916 and 1082-1095 in Discussion section) and in Table 3 the peculiar features of January were reported and explained. The occurrence of exceptional wind events is, unfortunately, not rare on the Ligurian coast. The January information has the same value of the other months and, in our opinion, it has to be treated together with the other data in the statistical analysis, because it represents a scenario that can occur.

Figure 7 includes January data, in the A and B panels. The observations are indicated by grey circles, as reported in the legend. We choose the multivariate analysis because in the environment the trend of a single variable is often associated to a number of forcings and not only to one. Therefore, this is the best way to discover significant relationships between station and/or variables.

Classical univariate analysis (such as correlation) was performed and the significant results reported in lines 770-775. They are rather few, indicating that, actually, the microparticle distribution depends on more forcings acting at the same time or, eventually, on variables that were not recorded in the present study. To test whether the environmental variables we recorded were responsible of the station features in terms of microparticle content of the sediment, we performed the multivariate RDA. As reported in Material and Methods section, in this case the microparticle features of each observation are response variables, and the environmental features (such as permeability and waves) explanatory variables.

Fig. 7A is the plot related to fibres, Fig. 7B to fragments and spheres. In the first case the January observations are scattered as the July ones, while April showed a higher similarity between stations. In the second panel, instead, December station 1 was very different from the other December stations. It means that the beach sites may be alternatively different or similar depending on the microparticle type. We think that the point is that, notwithstanding the rather scattered observations, the entire multivariate analysis shows that permeability and wave direction significantly explain the microparticle distribution. It would be more surprising if all the observations were always grouped by month. And also alarming, because it would mean that the microparticle input to the beach, different for each month, is so high to mask totally the morphodynamic differences of the sites.

Actually, the Fig. 7 has a statistical value only if linked to Tables 4-7. We can delete the Fig. 7 if it can bring the reader to misunderstand what the text reported. However, given that the significant differences (or similarities) between stations have been already reported describing and discussing the single parameters, we added few sentences in the Discussion section, as requested by the Reviewer. We highlighted that also in the plots the stations grouped depending on the microparticle abundance and

that, especially for fibres, the relationship with permeability was not only statistically but also visually rather clear.

Highlights to:

“Hydrodynamic forcing and sand permeability influence the distribution of anthropogenic microparticles in beach sediment”

by C. Misic, A. Covazzi Harriague, M. Ferrari

- Anthropogenic microparticles (Mps) were studied on a NW Mediterranean beach
- Mps abundance (416 ± 202 Mps kg^{-1}) and distribution were related to environmental characteristics
- Fibres were the main Mps morphology (>90%)
- Hydrodynamism (wave characteristics, rip current) and sediment permeability influenced fibre distribution
- Fragment accumulation depended on the efficiency of waves at removing stranded materials

1
2
3 **Hydrodynamic forcing and sand permeability influence the distribution of anthropogenic**
4 **microparticles in beach sediment.**
5
6
7
8

9 Cristina Mistic, Anabella Covazzi Harriague, Marco Ferrari
10
11
12

13
14 Department of Earth, Environment and Life Sciences, University of Genova, Genova, Italy
15
16
17
18
19
20
21
22
23

24 Corresponding author:
25

26 Cristina Mistic
27

28 Department of Earth, Environment and Life Sciences - University of Genova
29

30 Corso Europa 26, 16132 Genova, Italy
31
32

33 Phone: +3901035338224
34

35 e-mail: mistic@dipteris.unige.it
36
37
38
39
40
41
42
43
44
45
46
47
48
49
50
51
52
53
54
55
56
57
58
59

60
61
62 **Abstract**
63

64 The distribution of anthropogenic microparticles (Mps), such as plastic and natural fibres used in
65 textiles, in beach sediments was studied in a human-influenced pocket beach in Liguria (NW
66 Mediterranean Sea). Information on environmental parameters such as rainfall, hydrodynamic
67 characteristics and sediment texture was collected at the same time as the sediment samples. The
68 Mps (416 ± 202 Mps kg^{-1} on average) were mainly fibres (57-100%), while fragments and spheres
69 showed irregular abundances linked to the draining action of waves on the beach. Uni- and
70 multivariate statistical analyses highlighted that the different spatial and seasonal distribution of
71 fibres primarily depended on the action of the waves that force seawater into the sand, rather than
72 on sedimentation following depositional processes. Wave height and direction had a role in fibre
73 distribution in the sand, as well as sediment permeability and sorting. The occurrence of short-term
74 and spatially-localised hydrodynamic events such as rip currents were observed to influence the
75 abundance of fibres, overlapping the seasonal sequences of beach accretion and erosion that is
76 typical of the area and increasing fibre abundance by transporting those accumulated in the
77 sediments of the submerged beach during winter.
78
79
80
81
82
83
84
85
86
87
88
89
90
91
92
93
94
95

96 **Key-words:** Anthropogenic microparticles, Beach sediment, Hydrodynamic characteristics,
97 Sediment texture, NW Mediterranean.
98
99

1. Introduction

The diffusion of microparticles (Mps) of anthropogenic origin in the marine environment is a highly debated topic, especially with respect to what composes microplastics (i.e., plastic particles ranging from 20 μm to 5 mm, Barnes et al., 2009). According to the scientific literature, primary and secondary microplastics can be distinguished as follows. The first type includes items produced to be small, such as microbeads derived for personal-care products (Bergmann et al., 2015), precursors or by-products of plastic production (Costa et al., 2010), sandblasting, and industrial-cleaning products (Browne, 2015). The second type includes small items (fragments, fibres, films, etc.) coming from the deterioration, weathering and photo-degradation of macroplastics that were used or abandoned in the environment (Andrady, 2011; Barnes et al., 2009; Claessens et al., 2011; Hidalgo-Ruz et al., 2012).

Natural materials used in textiles are another source of anthropogenic Mps. They can be confused with common microplastic fibres and hold similar environmental concerns as both have been found to adsorb chemical pollutants (Ladewig et al., 2015). Information related to the distribution at sea of these materials is nearly absent (Song et al., 2015), although they can reach the environment following the same pathways as synthetic fibres before biodegradation takes place. In fact, fibres of natural origin, such as cotton and wool, are biodegradable (Chen and Burns, 2006; Ladewig et al., 2015), and they may achieve a rather high importance; in the seawater surface they may account for up to 85% of the total fibre abundance (e.g., the coastal area of South Korea, Song et al., 2015). The principal input of anthropogenic-derived fibres is due to the machine-washing of natural and synthetic textiles that enter into wastewater, yet cannot be retained by sewage treatment plants (Desforges et al., 2014). Both natural and synthetic materials that adsorb dissolved pollutants may have deleterious effects (Ladewig et al., 2015), but they may also be a threat because of the chemicals that are used to improve performance and dye textiles (Chen and Burns, 2006). Recent scientific literature concerning microplastics reports their influence on both individual organisms and food webs (Rochman et al., 2013). The small size of Mps facilitates intake by organisms

178
179
180 (Lusher et al., 2013; Remy et al., 2015). Thus, planktonic and benthic organisms may ingest
181
182 particles that accumulate in the water column and sediment (Deudero et al., 2014;
183
184 VanCauwenberghe et al., 2015; Wright et al., 2013). The consequence of ingestion of
185
186 anthropogenic-derived items could be the uptake of additives such as phthalates used to enhance
187
188 plastic performance and/or the uptake of adsorbed persistent organic pollutants (Teuten et al.,
189
190 2007). Other general negative impacts may be f mechanical in nature, such as suffocation or
191
192 reduction of feeding activity (Lusher, 2015).
193

194
195 Mps have been found in all environmental components, from the water column to the sediment.
196
197 Items denser than water may sink due to their physical and chemical features (Woodall et al., 2014),
198
199 but biofilm accrual often reduces the buoyancy of materials lighter than water, making them sink as
200
201 well (Andrady, 2011; Jorissen, 2014; Reisser et al., 2013; Zettler et al., 2013). Furthermore, wind
202
203 and currents may carry the items far from their production or site of last-use (Suaria and Aliani,
204
205 2014), thus contaminating rather pristine environments (Alomar et al., 2016). Data related to
206
207 plastics in the sediment have been published since the beginning of the 21st Century (Sanchez-Vidal
208
209 et al., 2018; Thompson et al., 2004), but few have dealt with coastal sites (Alomar et al., 2016;
210
211 Graham and Thompson, 2009; Palatinus et al., 2019). Little is known about seasonal variations and
212
213 temporal trends of natural fibres and microplastics on beaches (Browne et al., 2011; Song et al.,
214
215 2015; Stolte et al., 2015), although it has been estimated that microplastics contribute between 8 and
216
217 40% of the total weight of plastic in beach sediments on the Belgian coast (Van Cauwenberghe et
218
219 al., 2015).
220

221
222 Despite the rising number of published studies over the last decades, many marine areas worldwide
223
224 have not been extensively studied, including zones where a high abundance of anthropogenic Mps
225
226 is documented such as the Mediterranean Sea (Fossi et al., 2017; Suaria et al., 2016). The Ligurian
227
228 coast (NW Mediterranean Sea) hosts a large variety of human activities that are sources of Mps. A
229
230 clear influence of these items on the marine ecosystem has not been highlighted yet, but potential
231
232
233
234
235
236

237
238
239 threats of this kind of pollution should not be ignored, especially in densely populated areas such as
240
241 the eastern Ligurian Riviera.
242

243
244 As observed for macrodebris (Browne et al., 2010), small-scale hydrodynamic characteristics of
245
246 coastal areas may regulate the ability of Mps to enter the sediment. Therefore, local features such as
247
248 coast exposure, sea-storm frequency and intensity, rip current formation, and presence of groynes
249
250 and breakwaters may play a role in the accumulation of Mps in beach sediment. In order to
251
252 investigate the influence of these physical and morphological features, we performed a seasonal
253
254 sampling of sediment in a typical Ligurian pocket-beach, whose hydrodynamic and morphometric
255
256 characteristics have been previously studied (Schiaffino et al., 2015). Environmental data were
257
258 collected at the same time. Due to the extraction protocols used to isolate the anthropogenic Mps -
259
260 employed for the microplastic extraction and described below - our data primarily related to plastic
261
262 items. Nevertheless, the lack of confirmation by Fourier transform infrared spectroscopy (FT-IR)
263
264 of the actual composition of these items and the possibility that some samples may contain fibres
265
266 derived from natural material used in textiles, led us to call all our items Mps, even thou they are
267
268 potentially only plastic.
269
270

271
272 In this study, we focused on sea wave features (i.e., wave direction and wave height) to determine if
273
274 short-term and low-energy wave action on sampling days exerted an influence on Mps abundance
275
276 and distribution in the sand, and whether this influence was different from the longer-term, high-
277
278 energy wave action associated with sea storms. We also studied on the mean grain size,
279
280 homogeneity, and permeability of the beach sediment, to determine if these sedimentary
281
282 characteristics were related to the penetration of the Mps in the sediment.
283
284
285

286 **2. Material and Methods**

287 *2.1 Study area and position of the stations*

288
289
290 The Levanto beach is located on the eastern Ligurian coast (44°10.18' N, 9°36.73' E) (Fig. 1). The
291
292 Levanto beach is a NNW-SSE oriented pocket beach delimited by two promontories and
293
294

296
297
298 representing the seaward extension of the Ghiararo Creek catchment. The annual mean rainfall
299
300 during the period 1932-2016 was 1050.4 mm as measured at the Levanto weather station. The
301
302 coastline displays wave conditions typical of Liguria, with the most severe storms surging from the
303
304 south (Ferrari et al., 2006). The most frequent and intense storms come from the southwest. The
305
306 Levanto beach is a micro-tidal area with a maximum tidal excursion of about 30-40 cm (Schiaffino
307
308 et al., 2015).

309
310 The Levanto beach extends for approximately 800 m and its width ranges from 35 to 50 m (Fig. 1).
311
312 It is delimited, on its backside, by a continuous wall and touristic facilities. In its central section,
313
314 this wall is interrupted to allow the Ghiararo Creek to flow to the sea. This is a very short,
315
316 ephemeral water course and its water was not visible on the beach surface during the sampling
317
318 period.
319

320
321 Some artificial structures protect the beach from wave action. In the central sector, two groynes
322
323 delimit the beach portion that contained Stations 1, 2 and 3. This sector has experienced minor
324
325 erosion in recent years (Schiaffino et al., 2015). In front of this part of the beach, approximately 65
326
327 m far from the shore, submerged and detached breakwater approximately 100-m in length was built
328
329 to further protect the beach.
330

331
332 Station positions were located in order to determine whether the aforementioned local
333
334 hydrodynamic characteristics and potential environmental sources have a role in the Mps content of
335
336 the beach sand. Station 1 was placed at the creek outlet, whereas the Station 3 was placed on the
337
338 opposite side where, during periods of bad sea conditions (when waves come from the southwest), a
339
340 rip current is generally observed due to the interaction of the waves and the southernmost groyne.
341
342 Station 2 was located in the middle of the offshore breakwater. Station 4 was placed south of the
343
344 southernmost groyne, next to the outlet of a very small channel (less than 0.5 m wide) that presents
345
346 a low but rather constant discharge. Station 5 was only sampled twice. It was placed on the
347
348 southernmost part of the beach, in a site characterised by very different hydrodynamic conditions,
349
350 due to the shelter of the existing external seawall and rocky peninsula.
351
352
353
354

355
356
357 Besides the structures built at sea and along the backside of the beach, and the intense use of the
358 beach for bathing and sunbathing, other anthropogenic pressures are present in the area. In the
359 northern part, the touristic harbour is highly frequented by small boats. A sewage treatment plant is
360 located in the immediate outback, discharging north of the harbour. Beach replenishment in the
361 central area (Stations 1-4) occurs nearly every year. In 2017, it began in May before the beginning
362 of the touristic season, although the beach is frequented by tourists all year long. The sand used for
363 replenishment is of fluvial origin and is washed and analysed before placement to avoid the
364 presence of contaminants (<http://www.comune.levanto.sp.it>).
365
366
367
368
369
370
371
372
373
374

375 376 *2.2 Sampling* 377

378 The sampling took place during 2017 by season, i.e., January (winter), April (spring), July
379 (summer), and December (late autumn). Station 5 was sampled only in July and December.
380
381

382 The sediment samples were collected at the watermark of the higher wave for each survey date
383 following Claessens et al. (2011). Sediment was picked up with stainless-steel cores of 4 cm
384 diameter and carefully cleaned with prefiltered (0.45 µm pore size) deionised water. The sediment
385 was sampled from the surface to a depth of 5 cm (as recommended by the Joint Research Centre of
386 the European Commission, 2013) and the samples were placed into clean glass containers, to be
387 treated as described below. Four replicates were collected at each station, as in Thompson et al
388 (2004), with an overall mean weight equal to 123 ± 19 g for every sediment sample. The total
389 sediment volume of 63 ml per replicate was similar to the 50 ml of sediment collected for each
390 replicate by Browne et al. (2010) in a study of microplastic spatial patterns along the shoreline of
391 the Tamar Estuary (UK).
392
393
394
395
396
397
398
399
400
401
402
403

404 Data concerning rainfall and waves were recorded by the Meteo-Hydrological Observatory of the
405 Regione Liguria (OMIRL, <http://www.arpal.org.it>). Furthermore, sea conditions, consisting of wave
406 height and direction, were recorded on the sampling day, for the latest sea storm, and for the week
407 before sampling.
408
409
410
411
412
413

414
415
416 The wave attack from SW on the beach (mean wave direction observed in Levanto) was modelled
417
418 using Xbeach. This is a two-dimensional model that simulates wave propagation and its mean flow
419
420 (Roelvink et al., 2009). The simulated wave attacks are representative of calm and stormy
421
422 conditions (i.e. Hs registering around 0.2 m for calm-sea conditions and Hs registering about 2.0 m
423
424 for those of stormy sea conditions). The computational grid has been generated by merging
425
426 bathymetric field data collected in 2015 and the data related to deeper bathymetry supplied by the
427
428 Hydrographic Institute of the Italian Navy.
429
430
431
432

433 *2.3 Sample treatment and analysis*

434 *2.3.1 Mps extraction and analysis*

435
436 The equipment used for sample processing was washed with diluted HCl and rinsed with prefiltered
437
438 (0.45 μm) deionised water; all working surfaces were cleaned with alcohol. A white lab coat was
439
440 always worn while analyses were performed.
441
442
443

444 Sample analyses were based on the protocols described by Thompson et al. (2004), Hidalgo-Ruz et
445
446 al. (2012), and the Joint Research Centre of the European Commission (2013) for microplastics,
447
448 because no protocol was available in the literature for the extraction of natural fibres from sediment.
449
450 However, the Joint Research Centre of the European Commission (2013) considered that the
451
452 analytical approaches described are likely to capture other man-made particles.
453

454 Mps were extracted by density separation. A saturated solution of NaCl (density 1.2 g cm^{-3} ,
455
456 Thompson et al., 2004) and ZnCl_2 (density 1.6 g cm^{-3} , Imhof et al. 2012) was added to each
457
458 sample. Each solution was prefiltered (0.45 μm) to remove any particles that may contaminate the
459
460 sample. The NaCl solution was added to the sediment twice (200 ml + 200 ml), whereas the ZnCl_2
461
462 only once (200 ml), resulting in a three-step extraction. After each addition, the sediment was
463
464 shaken for 5 minutes; after 10 minutes, the supernatant was transferred to a glass container. Next,
465
466 100 ml HCl (Desforges et al, 2014) was added to the sample in order to digest residual organic
467
468 material. The concentration of HCl was 37%, therefore the final concentration was below 5%. This
469
470
471
472

473
474
475 concentration allowed the samples to be cleaned and analysed. We tested the effect of this HCl
476
477 concentration on textiles, and no change of colour or damage was observed, but a bleaching of the
478
479 coloured fibres cannot be excluded *a priori*. The action of hydrogen peroxide (H₂O₂), whose use
480
481 has already been suggested by other authors such as Stolte et al. (2015), was not enough to digest
482
483 the vegetal debris sometimes found in samples.
484

485
486 After 24 h digestion, the samples were filtered through mixed cellulose-ester filters (47 mm, 0.45
487
488 µm pore size). This procedure was performed under vacuum filtration by using a glass filtering
489
490 apparatus and rinsing carefully the containers with prefiltered (0.45 µm) deionised water.
491

492
493 The filters were placed in clean glass Petri dishes. Control samples, represented by filters subjected
494
495 to the same conditions as the samples under investigation but without sediment, were made every
496
497 time to evaluate laboratory background contamination expected from airborne particles. Each filter
498
499 was carefully inspected under a dissecting stereo microscope (Leica EZ4) with 30x magnification.
500
501 The Mps were identified according to morphological characteristics and physical properties (e.g.,
502
503 response to physical stress, whether they were bendable or soft, and colour) as reported in Hidalgo-
504
505 Ruz et al. (2012). Furthermore, they were counted and categorized into three broad categories:
506
507 fibres, fragments (including fragments and films), and spheres (i.e., pellets and all items that
508
509 showed a spherical shape). The dimension of some representative fragments and spheres and the
510
511 length of some typical fibres (e.g., the transparent ones) were determined with a Leica DFC290
512
513 stereomicroscope (magnification 90x) and associated Leica Application Suite (LAS) software to
514
515 image acquisition and elaboration. Due to the very small size (identified fibres were substantially
516
517 less than 2 mm in length, often approximately 0.1 mm long; the longest were too thin to be analysed
518
519 properly), it was not possible to analyse them with FT-IR spectroscopy and distinguish between
520
521 natural and synthetic materials.
522

523
524 Fibres were counted and divided by colour (transparent, black, blue, red, and violet), whereas
525
526 fragments and spheres were only counted. After subtracting the control values, the values were
527
528 expressed as Mps kg⁻¹ dry weight sediment.
529
530
531

532
533
534
535
536 *2.3.2 Sediment characteristics*
537

538 The sediment of each replicate, after extraction, was washed using freshwater to remove inorganic
539 salts, and then placed in a furnace (105°C) to dry for 24 h. Subsequently, the sediment texture was
540 investigated. A stack of stainless-steel sieves was used, from 0.063 to 16 mm (i.e. from -4 phi to +4
541 phi) mesh size. The sediment in the stack was shaken for 5 minutes and the sediment retained in
542 each sieve was weighed (Denver APX200 balance, d=0.1 mg) for the definition of the grain size.
543
544

545 Mean grain size, permeability, and sorting were calculated as follows:
546
547

548
549
550
551 Mean grain size (mm) = $(\phi_{16} + \phi_{50} + \phi_{84})/3$
552

553 where ϕ_{16} , ϕ_{50} , and ϕ_{84} represent the dimension of the 16th, 50th, and 84th percentile (Folk and
554 Ward, 1957)
555

556
557 Permeability (cm s⁻¹) = $(\phi_{90})^2 * c$
558

559 where ϕ_{90} represents the dimension of the 90th percentile of retained sediment and c a coefficient
560 equal to 0.011(Hazen, 1911); and
561

562
563
564 Sorting (phi) = $(\phi_{84} - \phi_{16})/4 + (\phi_{95} - \phi_5)/6.6$
565

566 where ϕ_{95} , ϕ_{84} , ϕ_{16} , and ϕ_5 represent the dimension of the 95th, 84th, 16th, and 5th percentile
567 (Folk and Ward, 1957).
568

569
570 The sediment organic content was also investigated. Protein and carbohydrate contents were
571 determined following the spectrophotometric methods of Hartree (1972) and Dubois et al. (1956)
572 using albumin and glucose solutions to calibrate the Jasco V-530 spectrophotometer.
573
574
575
576
577

578
579 *2.4 Statistical analyses*
580

581 A two-tailed *t*-test was used to verify the differences between stations in the same sampling for the
582 same variable, and a paired *t*-test was used to verify the differences among samplings over time.
583

584 Moreover, a Spearman-rank correlation was used to test the significance of the relationships among
585 variable trends (STATISTICA software). The redundancy analysis (RDA) (Zuur et al., 2007) was
586
587

591
592
593 applied on normalised data to verify the influence of the environmental variables on the total
594 abundance and colour of fibres and on the abundance of fragments and spheres using a Brodgar
595 2.5.6 package, 2011(Highland Statistics Ltd.). RDA is a form of constrained ordination that
596 examines how much of the variation in one set of variables explains the variation in another set of
597 variables. RDA is a direct gradient analysis technique which summarises linear relationships among
598 components of response variables (in this case the features of Mps) that are explained by a set of
599 explanatory variables (normalised mean grain size, permeability, carbohydrate and protein content,
600 and protein/carbohydrate ratios). The sampling season and the wave direction on the sampling day
601 and during the latest sea storm were nominal explanatory variables (ranked 0 or 1). Moreover, to
602 test the order of importance of the explanatory variables an automated forward selection model was
603 applied. First, the “marginal effects”, i.e., the variance expressed by one explanatory variable only,
604 were calculated. Then the “conditional effects” that showed the increase in the total sum of
605 eigenvalues after including a new variable during the forward selection, were calculated. Finally, a
606 permutation test was applied (number of permutations: 499) in order to test the null hypothesis, i.e.,
607 the explained variation is larger than a random contribution
608
609
610
611
612
613
614
615
616
617
618
619
620
621
622
623
624
625
626

627 **3. Results**

628 *3.1 Mps morphology*

629
630 In the sediment of the Levanto beach, a relevant dominance of fibres was observed. In most of the
631 samples they represented more than 90% of the observed Mps and, when present, fragments were
632 generally more abundant than spheres. The highest contribution of fragments and spheres to the
633 total ($41 \pm 3\%$) characterised the January sampling at Stations 3 and 4 (Table 1). Except for these
634 two stations (where fragments reached values up to 209 ± 190 fragments kg^{-1}), fragments and spheres
635 contributed $11 \pm 3\%$ during the January and April samplings (27 ± 8 and 31 ± 5 fragments kg^{-1} , 4 ± 3
636 and 1 ± 1 spheres kg^{-1} , respectively), whereas their contribution dropped to $1 \pm 1\%$ (ranging from 0
637 to 3%) in the July and December samplings. Fragment and sphere dimensions ranged between 0.05
638
639
640
641
642
643
644
645
646
647
648
649

650
651
652 and 0.5 mm. Fibres showed variable lengths and morphologies, as described in Section 3.2. No
653
654 significant relationships were found between the abundance of fibres and the overall quantity of
655
656 fragments and spheres at the same station and considering different seasons.
657
658

660 3.2 Fibre distribution and morphology

661
662 Fig. 2A reports the total abundance of fibres for each station on each sampling date. The same
663
664 station registered rather different values on the four sampling dates. For instance, in the January
665
666 sampling, Station 4 showed the lowest value recorded (124 ± 26 fibres kg^{-1}), which was
667
668 significantly lower than the values registered at Stations 1 and 3 on the same sampling date. On the
669
670 following sampling dates, the abundance of fibres increased, reaching a maximum value in
671
672 December (563 ± 51 fibres kg^{-1}), when it was higher than the values registered at the other stations
673
674 (significantly higher compared to Station 5, Fig. 2A). Station 1 showed the highest value in July
675
676 (893 ± 109 fibres kg^{-1}), which was significantly higher than Stations 3 and 5 on the same sampling
677
678 date (Fig. 2A). However, in the other samples the values were below 400 fibres kg^{-1} (significantly
679
680 lower than Station 3 in January). Among the stations sampled four times (Stations 1 through 4),
681
682 Station 3 reported the most stable values, ranging from 208 ± 98 fibres kg^{-1} in April to 499 ± 118
683
684 fibres kg^{-1} in December.
685
686

687
688 Among the fibres analysed, the transparent ones (Fig. 2A) were the most abundant in all of the
689
690 samples ($80 \pm 11\%$). January samplings showed the lowest contribution ($68 \pm 12\%$, Stations 1-4)
691
692 and July showed the highest ($90 \pm 7\%$ at Stations 1-4 and $85 \pm 11\%$ at Station 5).
693
694

695
696 The coloured fibres (Fig. 2B) also showed variable values at the same sites. Nevertheless, the most
697
698 abundant fibres were blue, contributing an average of $53 \pm 18\%$ for all the samplings, followed by
699
700 black ($20 \pm 13\%$), violet ($16 \pm 16\%$), and red ($11 \pm 9\%$). The highest contribution of the coloured
701
702 fibres to the total abundance was noticed in January ($32 \pm 12\%$); it was higher than the values
703
704 registered in July ($15 \pm 11\%$), December ($16 \pm 6\%$) and April ($20 \pm 10\%$).
705
706
707
708

709
710
711 Fibres were grouped into three classes depending on their length: small (from 0.1 to 0.5 mm),
712 medium (from 0.5 to 2 mm), and large (longer than 2 mm). Small fibres (averaging 304 ± 188 fibres
713 kg^{-1}) were significantly more abundant than medium (averaging 56 ± 39 fibres kg^{-1}) and large
714 (averaging 25 ± 19 fibres kg^{-1}) fibres (t-tests, $p < 0.001$). Fig. 3 shows the contribution of each class
715 grouped by colour (dark: blue + black, light: red + violet, and transparent). Temporal differences
716 were observed for the small transparent and violet fibres. They were more abundant in samples
717 taken in July and December, than in January and April (t-test, $p < 0.01$ and $p < 0.05$, respectively).
718 The transparent fibres of medium and large length had a cylindrical section, whereas the small
719 transparent fibres had flattened sections and were more curled than the large ones. Dark coloured
720 fibres had a cylindrical section as well as the smallest ones. The edges were net-cut in the
721 cylindrical fibres, whereas they were irregular in the flattened ones.
722
723
724
725
726
727
728
729
730
731
732
733
734
735
736

737 *3.3 Sediment features*

738
739 The sediment texture (Table 2) showed a rather high variability. Stations 1 and 2 showed the higher
740 mean grain size (4.9 ± 2.1 mm and 3.4 ± 2.0 mm, respectively). Station 5 showed the finest grain
741 size (0.4 ± 0.0 mm). The highest value was recorded in Station 1 in December, the lowest in Station
742 5 in July.
743
744
745
746

747 The sediment permeability (Table 2) was higher in January ($3.17 \pm 2.67 *10^{-2} \text{cm s}^{-1}$) and July (2.67
748 $\pm 2.49 *10^{-2} \text{cm s}^{-1}$) than in April ($0.47 \pm 0.44 *10^{-2} \text{cm s}^{-1}$) and December ($0.67 \pm 0.67 *10^{-2} \text{cm s}^{-1}$).
749 The highest mean value was recorded at Station 1 ($3.33 \pm 2.70 *10^{-2} \text{cm s}^{-1}$), and the lowest at
750 Station 5 ($0.04 \pm 0.02 *10^{-2} \text{cm s}^{-1}$).
751
752
753
754
755

756 The sediment sorting ranged between 0.73 ± 0.05 phi (moderately sorted) measured at Station 5 in
757 July and 2.12 ± 0.48 phi (very poorly sorted) at Station 1 in December (Table 2). All the stations in
758 January and April showed a poorly-sorted sediment, whereas higher variability and a dominance of
759 moderately-sorted sediment was observed for July and December. Stations 1 through 4 showed
760
761
762
763
764
765
766
767

768
769
770 similar mean values (from 1.29 ± 0.31 phi for station 3 to 1.36 ± 0.53 phi for station 1), and Station
771
772 5 (sampled only in July and December) showed the lowest value (0.78 ± 0.07 phi).
773

774 The sediment-permeability trends showed a significant and direct correlation with the abundance of
775 fibres ($r = 0.58$, $n = 18$, $p < 0.01$), whereas the sorting resulted in significant and inverse correlation
776 to the abundance of fibres ($r = -0.48$, $n = 18$, $p < 0.05$).
777
778

779
780 The organic matter content showed a general dominance of carbohydrates over proteins (Fig. 4).
781
782 The highest values were recorded in April, (on average $89.5 \pm 75.0 \mu\text{g g}^{-1}$ for carbohydrates and
783 $19.9 \pm 13.2 \mu\text{g g}^{-1}$ for proteins). They were higher than those documented in January (averaging 15.2
784 ± 10.3 and $5.6 \pm 5.7 \mu\text{g g}^{-1}$), July (on average $24.8 \pm 16.2 \mu\text{g g}^{-1}$ and $16.7 \pm 13.3 \mu\text{g g}^{-1}$) and
785 December (averaging $18.7 \pm 6.8 \mu\text{g g}^{-1}$ and $11.9 \pm 8.1 \mu\text{g g}^{-1}$). The correlation between
786 carbohydrates and proteins were significant ($r = 0.64$, $n = 18$, $p < 0.001$), but the organic matter did
787 not show any correlation with the abundance of fibres, fragments or spheres.
788
789
790
791
792
793
794
795
796
797

800 *3.4 Environmental features*

801

802 The mean wave height, the significant wave height, and the wave direction were recorded for the
803 day of sampling, for the latest sea storm, and for the week before the sampling (Table 3, Fig. 5A
804 and 5B). During sampling, the wave height was generally low, except for July when the significant
805 wave reached a value of 0.91 m. The lowest wave height was documented in January (lower than
806 10 cm). It was due to an exceptionally strong wind from 46°N (<http://www.arpal.org.it>) that
807 completely flattened the sea on the shore, suppressing wave action. Except for January, the
808 direction of the waves on the sampling days was from southwest.
809
810

811 Values of the mean wave height relate to the week before sampling, except the sea storm day. The
812 values were similar to those on the respective sampling days (in April and July, December showed
813 higher height) and the directions overlapped. Again, January showed different characteristics. The
814 week before sampling, they were clearly divided into two very different conditions (Table 3).
815
816
817
818
819
820
821
822
823
824
825
826

827
828
829 Sea storms generally occurred 2 to 4 days before samplings. The wave direction was similar for
830
831 January and July, while the sea storms of April and December came from the east (108°N) and
832
833 southeast (122°N), respectively. Wave heights on storm days were higher than 2 m (January and
834
835 December, Table 3) and showed lower values (1.50 ± 0.30 m) in July. The mean wave height in
836
837 April had the lowest value for any storm day (less than 1 m).
838

839
840 The wave propagation models (Fig. 6) in both simulated conditions have not shown significant
841
842 energy changes along the shoreline from Station 1 through Station 4. Only near station 5 was the
843
844 wave height close to zero. Rip currents were observed. In stormy sea conditions (Fig. 6A) two rip
845
846 currents were observed adjacent to the central groyne. Station 1 was located very close to the
847
848 groyne and was not directly influenced by these water movements. A third rip current, of weak
849
850 intensity, was observed near station 5. A strong rip current was present near station 3. The rip
851
852 current placed south of Station 1 was also present, although very weak, in calm-sea conditions (Fig.
853
854 6B).
855

856
857 The year 2017 was rather dry, with a total rainfall slightly higher than 750 mm vs approximately
858
859 1050 mm for the period 1932-2016 (Levanto weather station). The cumulative rainfall registered
860
861 over the 30 days before each sampling was 15 mm (0 - 10 mm per day) for January, 25 mm (0 - 10
862
863 mm per day) for April, 14 mm (0 - 9 mm per day) for July, and increased slightly in December for a
864
865 total of 73 mm, ranging between 0 and 22 mm per day.
866
867

868 869 *3.5 Multivariate statistical analysis* 870

871
872 The RDA showed that the influence of the environmental features was different for fibres and for
873
874 fragments and spheres. Fig. 7 reports the graphical outputs of the RDAs.
875

876
877 The RDA applied on fibres explained a rather high part of the variance (0.56, axis 1 explaining 29%
878
879 of the variance and axis 2 13%, Table 4) and showed that sediment permeability and wave direction
880
881 (during the day of sampling and during the latest sea storm) significantly influenced the distribution
882
883 and abundance of fibres over the beach (Table 5).
884
885

886
887
888 The RDA applied on fragments and spheres explained 0.53 of the variance (axis 1 47%, axis 2
889 6%, Table 6), but showed that only the wave direction during the sampling was significantly related
890 to the distribution of Mps on the shore (Table 7).
891
892
893
894
895

896 897 **4. Discussion**

898
899 The fragment and sphere abundance and the fibre abundance in the different samplings showed
900 relevant differences. However, no significant relationships were found between these two groups,
901 indicating that these Mps types may have mixed with the beach sediment following different
902 processes (Browne et al., 2011; Stolte et al., 2015). Therefore, we analysed them separately.
903
904
905
906

907 In January, the fragment and sphere abundance was rather high, with the highest fragment
908 abundance at Stations 3 and 4. Also macro-litter (such as packaging, ropes, funnels and highly
909 degraded plastic items) was found at Stations 3 and 4. This macro-litter accumulation was not
910 observed in the other samplings. The differences between the months are rather clear in the RDA
911 plot (Fig. 7B), where the first axis explains 47% of the variance and the January sites have been
912 separated from the observations made in the other months. The RDA highlighted that the abundance
913 of fragments and spheres may be significantly influenced by the action of waves on the sampling
914 day. Actually, wave direction and height on sampling days impeded accumulation. In fact, in
915 January, the strong northeast wind event that started about two days before sampling led to
916 negligible waves that did not have the force to drain stranded debris to sea, causing the relevant
917 abundance of fragments and spheres found.
918
919
920
921
922
923
924
925
926
927
928
929

930 The higher abundance of fragments and spheres in April than in December, considering that the
931 wave direction and height were similar, depended on the wave heights that occurred before the two
932 samplings. In fact, we observed lower values for wave height in April for both the regular regime
933 and in the sea-storm regime the week before each sampling (Table 3), while December showed
934 higher wave heights. The draining of fragments and spheres by the waves in the days before the
935 April sampling was less efficient than that of December. Part of these fragments and spheres may
936
937
938
939
940
941
942
943
944

945
946
947 have derived from those observed in January. On the whole, the abundance of fragments and
948
949 spheres was four times lower in April than in January, while no macro-litter was observed at
950
951 Stations 3 and 4 in April. Different patterns in the distribution and characterisation of micro and
952
953 macro-debris were previously observed by Browne et al. (2010), mainly related to wind action and
954
955 the density of the materials.
956

957
958 The RDA highlighted that fibre distribution and abundance were, instead, influenced by the
959
960 sediment permeability, the wave direction of the previous sea storms and the wave direction of the
961
962 sampling day. The distribution of the observations in the RDA plot reported in Fig. 7A points to the
963
964 significant relationship between the fibre abundance and permeability, already indicated by the
965
966 univariate analysis. The July stations showing the highest fibre abundances are grouped on the left
967
968 side of the first axis, where permeability presented the highest scores, while the samplings showing
969
970 the lowest fibre abundances (April observations and station 4 in January) are, instead, on the right
971
972 side of the axis, opposite to the permeability vector.
973

974
975 Huettel and Gust (1992), with their experiments in stirred chambers, have shown that penetration in
976
977 the sediment of small items such as algal cells depended on sediment permeability and dynamic
978
979 processes, such as water flushing. In our study, higher fibre abundance was found in the most
980
981 permeable sediments. The penetration of Mps into the sediment was influenced by grain size,
982
983 sorting and state of consolidation of sediments (Rusch and Huettel, 2000). In the Levanto beach, the
984
985 inverse correlation between abundance of fibres and sorting values indicated that fibres accumulate
986
987 mainly in homogeneous sediments. Station 5, although it was sampled only twice, showed the
988
989 lowest permeability, finest grain size, and low abundance of fibres. The wave height of this area
990
991 was generally low. The sheltered conditions allow for depositional processes of finer sediment grain
992
993 sizes but does not for fibres. This observation and the previous statistical evidence supported the
994
995 hypothesis that wave action led to a forced flushing of water into the sand, which may play a
996
997 relevant role in the distribution of fibres inside the beach.
998
999
1000
1001
1002
1003

1004
1005
1006 Waves were identified as an important parameter used in determining the fate of microparticles in
1007 the beach sediment. The waves were not uniform along the sampling sites because some Stations
1008 were protected by groynes and the submerged breakwater. In addition, wave direction at Levanto
1009 was primarily observed as coming from SW (Fig. 6). Therefore, we processed the hydrodynamic
1010 data in order to obtain a schematic diagram of the wave energy as well as direction along the shore
1011 in case of waves arriving from SW. The model results for low height of waves indicated the
1012 occurrence of a low-energy rip current in the area of station 1, possibly reducing the wave
1013 efficiency and thus also lowering the introduction in the sediment of the allochthonous particles
1014 floating into the water, as plastic ones. This current may have had a role in samples that were
1015 mainly taken in April and December, when the sampling-day wave on the shore had a mean height
1016 of 0.20 ± 0.02 m and 0.30 ± 0.05 m, respectively. In the April sampling, the fibre distribution for the
1017 area, which was influenced by the two groynes (stations 1 through 4) and partially protected by the
1018 submerged breakwater (stations 1 through 3) showed slightly lower values at Stations 1 and 2 than
1019 at Station 3, with an increase at Station 4. In December, the trend was similar; although the fibre
1020 abundance was higher. This difference may have different explanations, one of which could be
1021 related to previous hydrodynamic events such as the height of the storm-day waves that was lower
1022 for the month of April (0.90 ± 0.27 m) than for that of December (2.12 ± 0.15 m).

1023
1024
1025
1026
1027
1028
1029
1030
1031
1032
1033
1034
1035
1036
1037
1038
1039
1040
1041
1042 In July, the wave direction was registered as coming from the SW during the previous sea storm
1043 cycle and during the sampling, when we recorded the highest wave height on the shore (on average
1044 0.85 ± 0.07 m). Waves characterised at this height were known to interact with the submerged
1045 breakwater generating the transport of sediment on the beach and a strong rip current originating
1046 from the area of Stations 3 and 4. This was illustrated by the model output for high energy waves
1047 coming from SW and has also been reported in previous studies. Given the wave direction and the
1048 orientation of the groynes, Schiaffino et al. (2015) observed that wave heights approaching 1 m
1049 resulted in the selective erosion of the beach line in specific places, due to the temporary rip
1050 currents that moved sediment offshore. Therefore, in this case it was not a matter of a weak current

1063 affecting the particle penetration in the sediment, but sediment actually being physically removed.

1064
1065 This has led to a lower abundance of fibres at Stations 3 and 4 than at the Stations 1 and 2. The rip
1066
1067 current eroded some centimetres of sand, exposing the layers below. Jackson et al. (2014) showed
1068
1069 that waves, together with tide movements, had a role in burying or re-suspending particles, such as
1070
1071 invertebrate eggs, embedded in the sediment. The reworking of sediment reached 3 to 4 cm in the
1072
1073 sediment, depending on the combined action of wave and tidal movement.
1074
1075

1076
1077 In our study, the rather high mean grain size of Stations 1 through 4 implied that fibre penetration in
1078
1079 the sediment was not a matter of the top mm, but water flushing and particulate material transport
1080
1081 occurred over several cm. This was possible, at least in Stations 1 through 4, where the mean grain
1082
1083 size was higher than 2 mm, as observed previously for particulates in a neighbouring Ligurian
1084
1085 pocket beach (the Baia Blu Beach, located 25 km eastward and having the same exposure and
1086
1087 texture) (Misic and Covazzi Harriague, 2007). The ability of Mps such as microplastics to penetrate
1088
1089 the beach sediment was previously observed by Carson et al. (2011), who found microplastics down
1090
1091 to 25 cm in the sand, although 50% was observed in the topmost 5 cm. Therefore, the fibre
1092
1093 contamination at Station 3 may be the result of previous infiltration processes and/or the transport in
1094
1095 the deeper layers due to the waves, facilitated by the coarse grain size.
1096
1097

1098
1099 In the case of higher waves (reaching offshore heights of nearly 3 m), the influence of submerged
1100
1101 breakwater was clear in the model output, where the area facing station 3 showed an increased wave
1102
1103 energy compared to the other Stations. Station 5, due to its sheltered position, did not demonstrate
1104
1105 these variation of wave energy and influence because the energy that was sustaining particle
1106
1107 penetration in the sediment always remained low, and therefore it showed low fibre abundance.
1108
1109

1110
1111 Also, the January sampling was preceded by a sea storm from a southwest direction, but the
1112
1113 following distribution of the fibres on the beach had a different pattern, with the highest value in
1114
1115 Station 3 that, in July, showed the lowest fibre abundance. This difference was due to the peculiar
1116
1117 wind-wave conditions after the storm event (as indicated by the significant influence of the wave
1118
1119 direction on sampling days highlighted by the RDA), that is the presence of the aforementioned
1120
1121

1122
1123
1124 exceptional northeast wind, which completely changed the wave direction, prevented the formation
1125 of the rip current and, consequently, resulted in a different fibre distribution.
1126

1127
1128 Most of the fibres were transparent in every season and small with curled shapes, especially in July
1129 and December. A small dimension (often below 0.3 mm) was also common also in coastal
1130 sediments of Croatia in the Adriatic Sea (Palatinus et al., 2019). The modification of the mean
1131 abundance and dimension of fibres registered after the first two samplings may have a seasonal
1132 explanation. In particular, the sharp increase recorded in July was associated with the recreational
1133 activities on the beach (Stolte et al., 2015) and in the neighbouring touristic harbour, both of which
1134 are generally known to increase the release of microplastics into seawater (Andrady, 2011;
1135 Desforages et al., 2014). Harbour sediments were also considered as reservoirs for pollutants due to
1136 the structure of the harbour itself in that it reduces water exchange with the area outside of the
1137 harbour (Claessens et al., 2013). An increase in vessel movements in the summer may cause
1138 resuspension of sediments and recirculation of settled particles, which may escape the harbour
1139 structure and be transported along the coast towards SE, as indicated by the model output for waves
1140 coming from SW. This phenomenon was observed in similar Ligurian touristic harbours, that in
1141 summer showed higher turbidity and concentrations of particulate matter, previously accumulated
1142 in the sediment (Misic and Covazzi Harriague, 2009).
1143
1144
1145
1146
1147
1148
1149
1150
1151
1152
1153
1154
1155
1156
1157
1158

1159
1160 The coloured fibres in the Levanto beach were mainly blue, as recorded by Stolte et al. (2015) for
1161 the Baltic Sea beaches. As these authors observed, it is possible that dark-coloured particles are
1162 more visible than light-coloured ones to the observer, thus causing an underestimation of the
1163 abundance of some category of coloured fibres.
1164
1165
1166
1167

1168
1169 The beach spring replenishment carried out in May, that covered the resident sand, was ineffective
1170 at increasing Mps abundance because the allochthonous sand was washed and analysed before
1171 loading onto the shore to avoid the introduction of pollutants. On the other hand, it is known that
1172 fibres are more abundant at coastal sites than offshore because they derive from the drainage of
1173 municipal wastewater (Alomar et al., 2016; Desforages et al., 2014). Machine washing of clothes is a
1174
1175
1176
1177
1178
1179
1180

1181
1182
1183 major source of fibres (Browne et al., 2011) that are discharged to the sea via pipes. At Levanto, the
1184 pipe was placed north of the touristic port, in an area where the littoral drift carries the inorganic
1185 particulate materials, and therefore, also Mps, from west to east (Schiaffino et al., 2015), allowing
1186 the released fibres to reach the shore or to sink into the sediment in front of the beach. Thus, water
1187 movement able to move submerged sediment and carry it to the coast may represent an input of
1188 Mps to the beach, given that deep sediments (Pham et al., 2014; Sanchez-Vidal et al., 2018;
1189 Woodall et al., 2014) and coastal sediments (Alomar et al., 2016) are sinks for anthropogenic Mps.
1190 Beaches experience seasonal variations related to wave energy (Short, 1979). In the Ligurian Sea
1191 during the winter months (characterised by high wave energy), the backshore is affected by a
1192 diffused erosive sequence of sediment, whereas in the summer (low wave energy), it is subjected to
1193 a depositional sequence. It is possible that the July sampling recorded general accretion on the
1194 beach of sediment and fibres, whose transport was promoted by the morphodynamic evolution. The
1195 increase of smaller, curled, and frayed transparent fibres suggests that they may originate from the
1196 mechanical-abrasion process carried out on larger plastic items by waves in the submerged
1197 sediment during the aforementioned erosive sequence, a process that may develop for several
1198 months during the winter period.

1200
1201
1202
1203
1204
1205
1206
1207
1208
1209
1210
1211
1212
1213
1214
1215
1216
1217
1218
1219
1220
1221
1222
1223
1224
1225
1226
1227
1228
1229
1230
1231
1232
1233
1234
1235
1236
1237
1238
1239
Another hypothesis was that the fibres entered the beach carried by Ghiararo Creek water, whose
mouth was next to Station 1. Its flowing water was not visible during samplings, but it may have
had a feeble subsurface flow through the sand and gravel. In the Ligurian area the continental inputs
are low and irregular, virtually absent during the summer. This was particularly true for 2017,
which was characterised by a lower cumulative rainfall than the average value during the period
1932-2016. The January-July period was homogeneously dry, but the Mps abundance showed
significant variations and reached rather high values, higher than those recorded in December after
an increase of rainfall. These trends contrast with the observation that continental input may move
large amounts of materials to the coastal area (Derraik, 2002).

1240
1241
1242 A biological effect, i.e., the retention of Mps in organic materials suspended in seawater, was not
1243
1244 likely, nor was an eventual chemical or mechanical binding of Mps with autochthonous organic
1245
1246 material on the beach. In this study, we did not find any significant correlation between
1247
1248 carbohydrate and protein content in sediments and the distribution of fibres or fragments. The
1249
1250 sedimentary organic matter was related to natural biological processes, as the detected
1251
1252 carbohydrates derived mainly from vegetal detritus which dominated on the protein content found
1253
1254 in the sediment. In April, organic matter showed the highest values, primarily due to primary
1255
1256 production processes in the seawater (Misic and Covazzi Harriague, 2008), whereas the Mps
1257
1258 showed their lowest abundance.
1259
1260

1261 1262 1263 **5. Conclusions**

1264
1265 As nearly all Ligurian beaches, the Levanto beach showed a strong anthropogenic influence, mainly
1266
1267 due to urbanisation and touristic activities. The building of artificial structures, such as the groynes
1268
1269 and the harbour, modified the natural sediment balance of the shore and introduced allochthonous
1270
1271 materials such as the Mps we studied into the coastal system. Actually, the origin of the Mps was
1272
1273 not determined, although for fibres, it is likely related to the input coming from the wastewater
1274
1275 carried to the sea via a pipe located in the northern part of the study area. These fibres may
1276
1277 accumulate in the submerged sediment all year along, and may be re-suspended and introduced to
1278
1279 the beach sand during the summer via the natural accretion sequence characteristic of this season,
1280
1281 with addition to vessel movements in the touristic harbour. The role of rainfall and of continental
1282
1283 input was not observed, likely due to the very dry regime of the sampled year. The abundance and
1284
1285 distribution of the fragments and spheres and of the fibres were mainly driven by hydrodynamic
1286
1287 characteristics that in this area were modified by the anthropogenic structures built offshore and
1288
1289 along the shore. This led to significant variations in the abundances of the Mps in the stations in the
1290
1291 four samplings, despite the rather low extension of the beach. The Levanto beach is predominantly
1292
1293 exposed to waves from the south. The southwest sector is the source of the most intensive and
1294
1295
1296
1297
1298

1299
1300
1301 frequent storms, therefore it is possible that these conditions promote the preferential penetration of
1302
1303 Mps in some sectors of the beach.
1304
1305
1306
1307
1308
1309

1310 **Acknowledgements**

1311
1312 We thank D. Barbieri for assistance in the field work and sample preparation. This research did not
1313
1314 receive any specific grant from funding agencies in the public, commercial, or not-for-profit sectors.
1315
1316
1317

1318 **References**

- 1319
1320 Alomar, C., Estarellas, F., Deudero, S., 2016. Microplastics in the Mediterranean Sea: Deposition in
1321
1322 coastal shallow sediments, spatial variation and preferential grain size. *Mar. Environ. Res.*
1323
1324 115, 1-10.
1325
1326
1327 Andradý, A. L., 2011. Microplastics in the marine environment. *Mar. Pollut. Bull.* 62, 1596-1605.
1328
1329 Barnes, D.K.A., Galgani, F., Thompson, R.C., Barlaz, M., 2009. Accumulation and fragmentation
1330
1331 of plastic debris in global environments. *Philos. Trans. R. Soc. B* 364, 1985–1998.
1332
1333 Bergmann, M., Gutow, L., Klages, M., 2015. *Marine Anthropogenic Litter*. Springer.
1334
1335 Browne, M.A., 2015. Sources and pathways of microplastic to habitats. In: Bergmann, M., Gutow,
1336
1337 L., Klages, M. (Eds.), *Marine anthropogenic litter*. Springer, Berlin, 229-244.
1338
1339 <http://dx.doi.org/10.1007/978-3-319-16510-3>.
1340
1341
1342 Browne, M.A., Crump, P., Niven, S.J., Teuten, E., Tonkin, A., Galloway, T., Thompson, R., 2011.
1343
1344 Accumulation of microplastic on shorelines worldwide: sources and sinks. *Environ. Sci.*
1345
1346 *Technol.* 45, 9175–9178.
1347
1348 Browne, M.A., Galloway, T.S., Thompson, R., 2010. Spatial patterns of plastic debris along
1349
1350 estuarine shorelines. *Environ. Sci. Technol.* 44, 3404–3409.
1351
1352
1353
1354
1355
1356
1357

- 1358
1359
1360 Carson, H.S., Colbert, S.L., Kaylor, M.J., McDermid, K.J., 2011. Small plastic debris changes
1361
1362 water movement and heat transfer through beach sediments. *Mar. Pollut. Bull.* 62, 1708–
1363
1364 1713.
1365
1366
1367 Chen, H.-L., Burns, L.D., 2006. Environmental analysis of textile products. *Cloth.Text. Res. J.* 24,
1368
1369 248-261.
1370
1371 Claessens, M., Van Cauwenberghe, L., Vandegehuchte, M.B., Janssen, C.R., 2013. New techniques
1372
1373 for the detection of microplastics in sediments and field collected organisms. *Mar. Pollut.*
1374
1375 *Bull.* 70, 227–233.
1376
1377
1378 Costa, M.F., Ivar do Sul, J.A., Silva-Cavalcanti, J.S., Araujo, M.C.B., Spengler, A., Tourinho, P.S.,
1379
1380 2010. On the importance of size of plastic fragments and pellets on the strandline: a
1381
1382 snapshot of a Brazilian beach. *Environ. Monit. Assess.* 168 (1-4), 299e304.
1383
1384
1385 Derraik, J.G.B., 2002. The pollution of the marine environment by plastic debris: a review. *Mar.*
1386
1387 *Pollut. Bull.* 44, 842-852.
1388
1389
1390 Desforges, J.-P.W., Galbraith, M., Dangerfield, N., Ross, P.S., 2014. Widespread distribution of
1391
1392 microplastics in subsurface seawater in the NE Pacific Ocean. *Mar. Pollut. Bull.* 74, 94-99.
1393
1394
1395 Deudero, S., Nadal, M.A., Estarellas, F., Alomar, C., 2014. Microplastic exposure in pelagic fishes
1396
1397 and holothurians: a Mediterranean case study. In: 2nd International Ocean Research
1398
1399 Conference. Barcelona 17-21 November 2014.
1400
1401
1402 Dubois, M., Gilles, K.A., Hamilton, J.K., Rebers, P.A., Smith, F., 1956. Colorimetric method for
1403
1404 determination of sugars and related substances. *Anal. Chem.* 39, 350-356.
1405
1406
1407 Ferrari, M., Bolens, S., Bozzano, A., Fierro, G., Gentile, R., 2006. The port of Genoa-Voltri
1408
1409 (Liguria, Italy): a case of updrift erosion. *Chem. Ecol.* 22, 361–369.
1410
1411
1412 Folk, R., Ward, W.C., 1957. Brazos River bar (Texas): a study in the significance of grain size
1413
1414 parameters. *J. Sediment. Res.* 27, 3-26.
1415
1416 Fossi, M.C., Romeo, T., Bainsi, M., Panti, C., Marsili, L., Campani, T., Canese, S., Galgani, F.,
Druon, J.-N., Airoidi, S., Taddei, S., Fattorini, M., Brandini, C., Lapucci, C., (2017) Plastic

1417
1418
1419 debris occurrence, convergence areas and fin whales feeding ground in the Mediterranean
1420
1421 Marine Protected Area Pelagos Sanctuary: a modeling approach. *Front. Mar. Sci.* 4, 167.
1422
1423 doi: 10.3389/fmars.2017.00167
1424

1425
1426 Graham, E.R., Thompson, J.T., 2009. Deposit- and suspension-feeding sea cucumbers
1427
1428 (Echinodermata) ingest plastic fragments. *J. Exp. Mar. Biol. Ecol.* 368, 22-29.
1429
1430 <http://dx.doi.org/10.1016/j.jembe.2008.09.007>.
1431

1432 Hazen, A., 1911. Discussion: dams on sand foundations. *T. Am. Soc. Civ. Eng.* 73, 199.
1433

1434 Hidalgo-Ruz, V., Gutow, L., Thompson, R.C., Thiel, M., 2012. Microplastics in the marine
1435
1436 environment: a review of the methods used for identification and quantification. *Environ.*
1437
1438 *Sci. Technol.* 46, 3060–3075.
1439

1440
1441 Hartree, E.F., 1972. Determination of proteins: a modification of the Lowry method that gives a
1442
1443 linear photometric response. *Anal. Biochem.* 48, 422–427.
1444

1445 Huettel, M., Gust, G., 1992. Impact of bioroughness on interfacial solute exchange in permeable
1446
1447 sediments. *Mar. Ecol. Prog. Ser.* 89, 253–267.
1448

1449 Imhof, H. K., Schmid, J., Niessner, R., Ivleva, N. P., Laforsch, C., 2012. A novel, highly efficient
1450
1451 method for the separation and quantification of plastic particles in sediments of aquatic
1452
1453 environments. *Limnol. . Oceanogr.: Methods* 10, 524-537.
1454

1455 Jorissen, F.J., 2014. Colonization by the benthic foraminifer *Rosalina (Tretomphalus) concinna* of
1456
1457 Mediterranean drifting plastics in CIESM 2014. In: Briand, F. (Ed.), *Marine litter in the*
1458
1459 *Mediterranean and Black Seas*. CIESM Publisher, Monaco, p. 180. CIESM Workshop
1460
1461 Monograph n. 46.
1462
1463

1464 Joint Research Centre of the European Commission - MSFD technical subgroup on marine litter,
1465
1466 2013. *Guidance on Monitoring of Marine Litter in European Seas*. Luxembourg:
1467
1468 Publications Office of the European Union,ISSN 1831-9424.54 doi:10.2788/99475
1469

1470 Ladewig, S.M., Bao, S., Chow, A.T., 2015. Natural Fibers: A Missing Link to Chemical Pollution
1471
1472 Dispersion in Aquatic Environments. <http://dx.doi.org/10.1021/acs.est.5b04754>.
1473
1474
1475

- 1476
1477
1478 Lusher, A L., McHugh, M., Thompson, R.C., 2013. Occurrence of microplastics in the
1479 gastrointestinal tract of pelagic and demersal fish from the English channel. *Mar. Pollut.*
1480 *Bull.* 67, 94-99. <http://dx.doi.org/10.1016/j.marpolbul.2012.11.028>.
1481
1482
1483
1484
1485 Lusher, A., 2015. Microplastics in the marine environment: distribution, interactions and effects. In:
1486 Bergmann, M., Gutow, L., Klages, M. (Eds.), *Marine anthropogenic litter*. Springer, Berlin,
1487 245-307. <http://dx.doi.org/10.1007/978-3-319-16510-3>.
1488
1489
1490
1491 Mistic, C., Covazzi Harriague, A., 2007. Enzymatic activity and organic substrates on a sandy beach
1492 of the Ligurian Sea (NW Mediterranean) influenced by anthropogenic pressure. *Aquatic*
1493 *Microbial Ecology* 47, 239-251.
1494
1495
1496
1497 Mistic, C., Covazzi Harriague, A., 2009. Organic matter characterisation and turnover in the
1498 sediment and seawater of a tourist harbour. *Mar. Environ. Res.* 68, 227-235.
1499
1500
1501
1502 Mistic, C., Covazzi Harriague, A., 2008. Organic matter recycling in a shallow coastal zone (NW
1503 Mediterranean): the influence of local and global climatic forcing and organic matter lability
1504 on hydrolytic enzyme activity. *Cont. Shelf Res.* 28, 2725–2735.
1505
1506
1507
1508 Palatinus, A., Kovač Viršek, M., Robič, U., Grego, M., Bajt, O., Šiljić, J., Suaria, G., Liubartseva,
1509 S., Coppini, G., Peterlink, M., 2019. Marine litter of the Croatian part of the middle Adriatic
1510 Sea: simultaneous assessment of floating and seabed macro e micro litter abundance and
1511 composition. *Mar. Pollut. Bull.* 139, 427-439.
1512
1513
1514
1515
1516 Pham, C.K., Ramirez-Llodra, E., Alt, C.H.S., Amaro, T., Bergmann, M., Canals, M., Company,
1517 J.B., Davies, J., Duineveld, G., Galgani, F., Howell, K.L., Huvenne, V.A.I., Isidro, E., Jones,
1518 D.O.B., Lastras, G., Morato, T., Gomes-Pereira, J.N., Purser, A., Stewart, H., Tojeira, I.,
1519 Tubau, X., Van Rooij, D., Tyler, P.A., 2014. Marine litter distribution and density in
1520 European seas, from the shelves to deep basins. *PLoS One* 9, e95839.
1521
1522
1523
1524
1525
1526
1527 Reisser, J., Shaw, J., Wilcox, C., Hardesty, B.D., Proietti, M., Thums, M., Pattiaratchi, C., 2013.
1528 Marine plastic pollution in waters around Australia: characteristics, concentrations, and
1529 pathways. *PLoS One* 8, e80466. <http://dx.doi.org/10.1371/journal.pone.0080466>.
1530
1531
1532
1533
1534

- 1535
1536
1537 Remy, F., Collard, F., Gilbert, B., Compère, P., Eppe, G., Lepoint, G., 2015. When microplastic is
1538 not plastic: the ingestion of artificial cellulose fibers by macrofauna living in seagrass
1539 macrophytodetritus. *Environ. Sci. Technol.* 49, 11158–11166.
1540
1541 <http://dx.doi.org/10.1021/acs.est.5b02005>.
1542
1543
1544
1545
1546 Rochman, C.M., Hoh, E., Kurobe, T., Teh, S.J., 2013. Ingested plastic transfers hazardous
1547 chemicals to fish and induces hepatic stress. *Sci. Rep.* 3 (3263).
1548
1549 <http://dx.doi.org/10.1038/srep03263>.
1550
1551
1552 Roelvink, D., Reniers, A., Van Dongeren, A., de Vries, J. v. T., McCall, R., Lescinski, J., 2009.
1553
1554 Modelling storm impacts on beaches, dunes and barrier islands. *Coast. Eng.* 56, 1133–1152.
1555
1556
1557 Rush, A., Huettel, M., 2000. Advective particle transport into permeable sediments - evidence from
1558 experiments in an intertidal sandflat. *Limnol. Oceanogr.* 45, 525-533
1559
1560
1561 Sanchez-Vidal, A., Thompson, R.C., Canals, M., de Haan, W.P., 2018. The imprint of microfibrils
1562 in southern European deep seas. *PlosONE* 13 (11), e0207033.
1563
1564
1565 Schiaffino, C. F., Dessy, C., Corradi, N., Fierro, G., Ferrari, M., 2015. Morphodynamics of a gravel
1566 beach protected by a detached low-crested breakwater. The case of Levanto (eastern
1567 Ligurian Sea, Italy). *Ital. J. Eng. Geol. Environ.* 1, 31-39.
1568
1569
1570
1571 Short, A.D., 1979. Wave power and beach stages: A global model. *Proc. 16th Conf. Coastal*
1572 *Engineering, Hamburg*, pp. 1145-1162.
1573
1574
1575 Song, Y.K., Hong, S.H., Jang, M., Han, G.M., Rani, M., Lee, J., Shim, W.J., 2015. A comparison of
1576 microscopic and spectroscopic identification methods for analysis of microplastics in
1577 environmental samples. *Mar. Pollut. Bull.* 93, 202–209.
1578
1579 <http://dx.doi.org/10.1016/j.marpolbul.2015.01.015>.
1580
1581
1582
1583
1584 Stolte, A., Forster, S., Gerds, G., Schubert, H., 2015. Microplastic concentrations in beach
1585 sediments along the German Baltic coast. *Mar. Pollut. Bull.* 99: 216–229
1586
1587
1588 Suaria, G., Aliani, S., 2014. Floating debris in the Mediterranean sea. *Mar. Pollut. Bull.* 86, 494-
1589 504. <http://dx.doi.org/10.1016/j.marpolbul.2014.06.025>.
1590
1591
1592
1593

- 1594
1595
1596 Suaria, G., Avio, C.G., Mineo, A., Lattin, G.L., Magaldi, M.G., Belmonte, G., Moore, C.J., Regoli,
1597
1598 F., Aliani, S. 2016. The Mediterranean Plastic Soup: synthetic polymers in Mediterranean
1599
1600 surface waters. *Sci. Rep.* 6, 37551. doi: 10.1038/srep37551
1601
1602
1603 Teuten, E.L., Rowland, S.J., Galloway, T.S., Thompson, R.C., 2007. Potential for plastics to
1604
1605 transport hydrophobic contaminants. *Environ. Sci. Technol.* 41, 7759–7764.
1606
1607 Thompson, R.C., Olsen, Y., Mitchell, R.P., Davis, A., Rowland, S.J., John, A.W.G., McGonigle, D,
1608
1609 Russel., A.E., 2004. Lost at sea: where is all the plastic? *Science* 304 (5672), 838.
1610
1611 Van Cauwenberghe, L., Claessens, M., Vandegehuchte, M., Janssen, C.R., 2015. Microplastics are
1612
1613 taken up by mussels (*Mytilus edulis*) and lugworms (*Arenicola marina*) living in natural
1614
1615 habitats. *Environ. Pollut.* 199, 10-17.
1616
1617
1618 Woodall, L.C., Sanchez-Vidal, A., Canals, M., Paterson, G.L.J., Coppock, R., Sleight, V.,
1619
1620 Calafat, A., Rogers, A.D., Narayanaswamy, B.E., Thompson, R.C., 2014. The deep sea is a
1621
1622 major sink for microplastic debris. *R. Soc. Open Sci.* 1, 140317.
1623
1624 <http://dx.doi.org/10.1098/rsos.140317>.
1625
1626
1627 Wright, S.L., Thompson, R.C., Galloway, T.S., 2013. The physical impacts of microplastics on
1628
1629 marine organisms: a review. *Environ. Pollut.* 178, 483-492.
1630
1631 Zettler, E.R., Mincer, T.J., Amaral-Zettler, L.A., 2013. Life in the “plastisphere”: microbial
1632
1633 communities on plastic marine debris. *Environ. Sci. Technol.* 47, 7137-7146.
1634
1635 <http://dx.doi.org/10.1021/es401288x>.
1636
1637 Zuur, A.F., E.N., Ieno, G.M., Smith, 2007. *Analysing ecological data*. Springer, New York.
1638
1639
1640
1641
1642
1643
1644
1645
1646
1647
1648
1649
1650
1651
1652

1653
1654
1655 **Captions to figures**
1656

1657 Fig. 1. Study area and location of Stations 1 -5. The dotted line denotes the beach width, delimited
1658 by a continuous wall interrupted at the mouth of Ghiararo Creek.
1659

1660 Fig. 2. Abundance \pm sd (fibres kg^{-1}) of (A) total fibres and transparent fibres. Significant differences
1661 (t-test, $p < 0.05$) for the total number of fibres among stations referred to the same sampling are
1662 indicated by the letters located on the histogram (the same letter means significant difference among
1663 stations); (B) coloured fibres.
1664

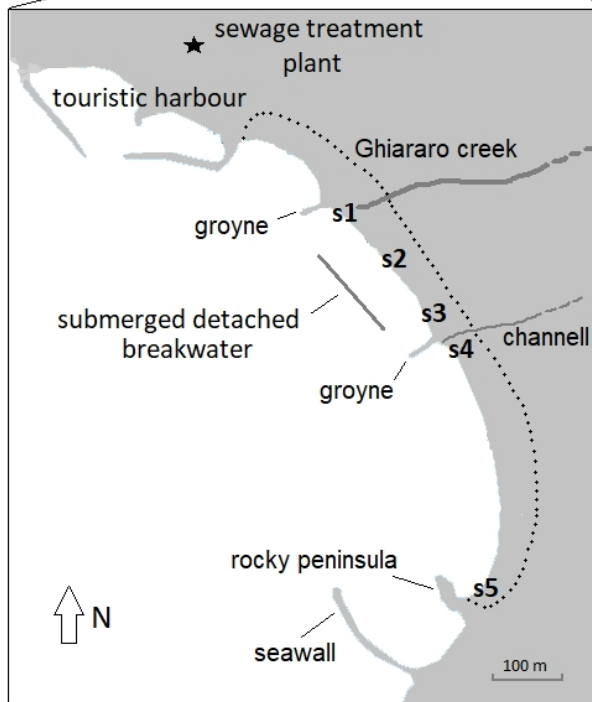
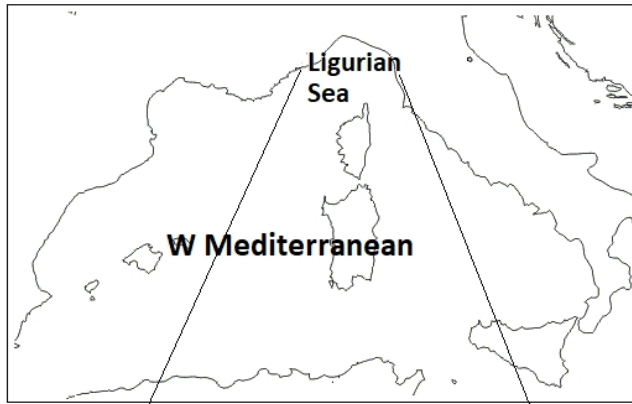
1665 Fig. 3. Size-class distribution of the coloured and transparent fibres: small (0.1 - 0.5 mm), medium
1666 (0.5 - 2 mm), large (larger than 2 mm). Dark colour: black and blue fibres, light colour: red and
1667 violet fibres.
1668

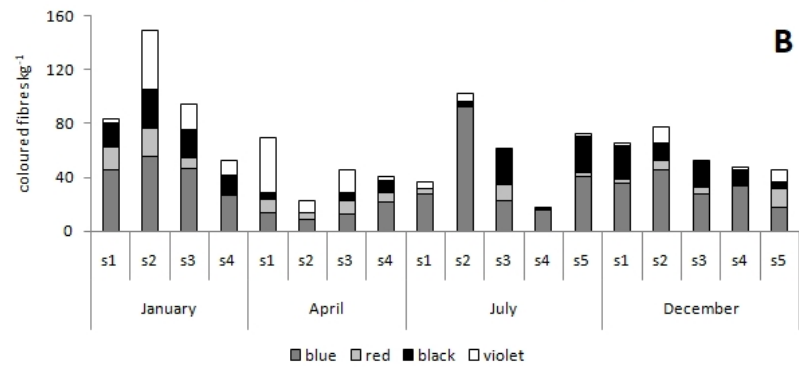
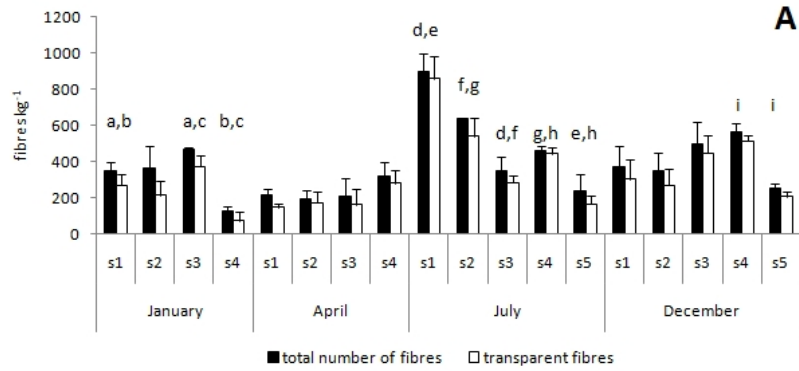
1669 Fig. 4. Sediment content \pm sd ($\mu\text{g g}^{-1}$) of carbohydrates and proteins.
1670

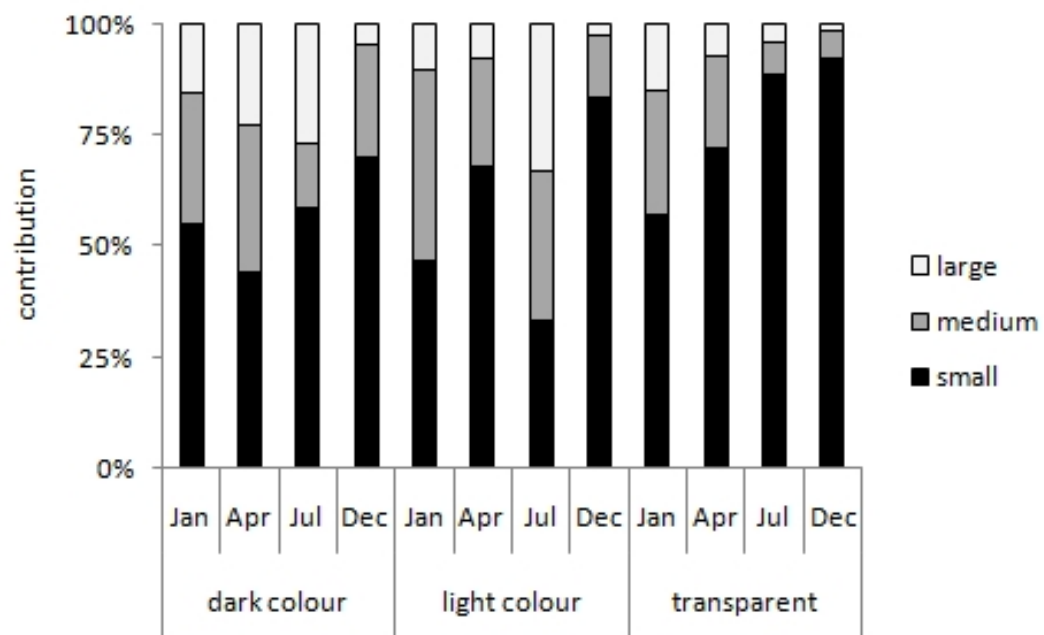
1671 Fig. 5. Characteristics of the waves on the sampling days (A) and for the latest sea storm (B). The
1672 vectors indicate the mean direction of waves, which were strongly related to wind direction.
1673

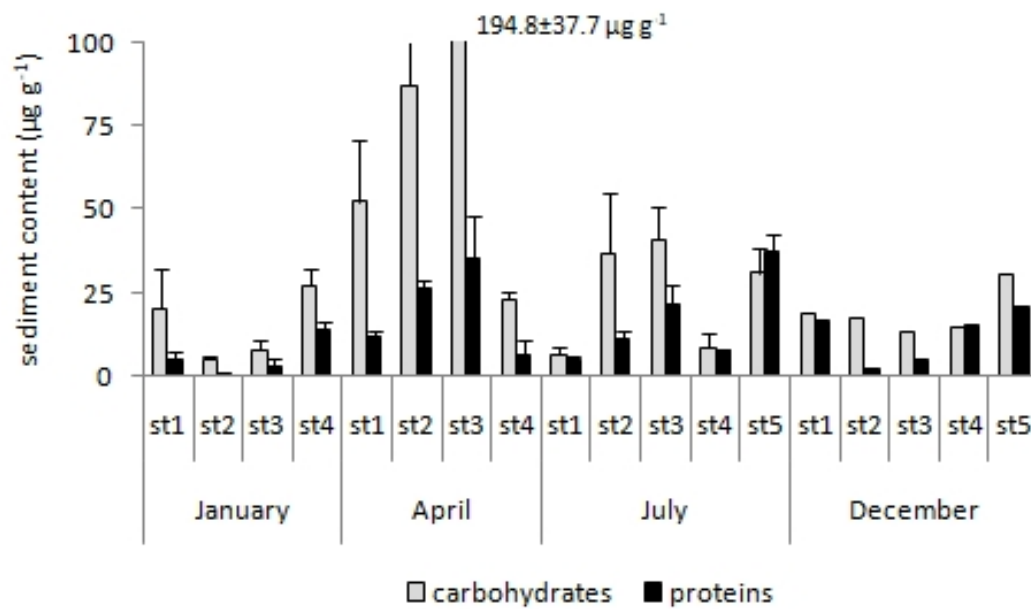
1674 Fig. 6. Outputs of the Xbeach model for waves coming from SW. A: storm-like wave height, B:
1675 calm-sea conditions. Coloured legends report the wave height (m).
1676

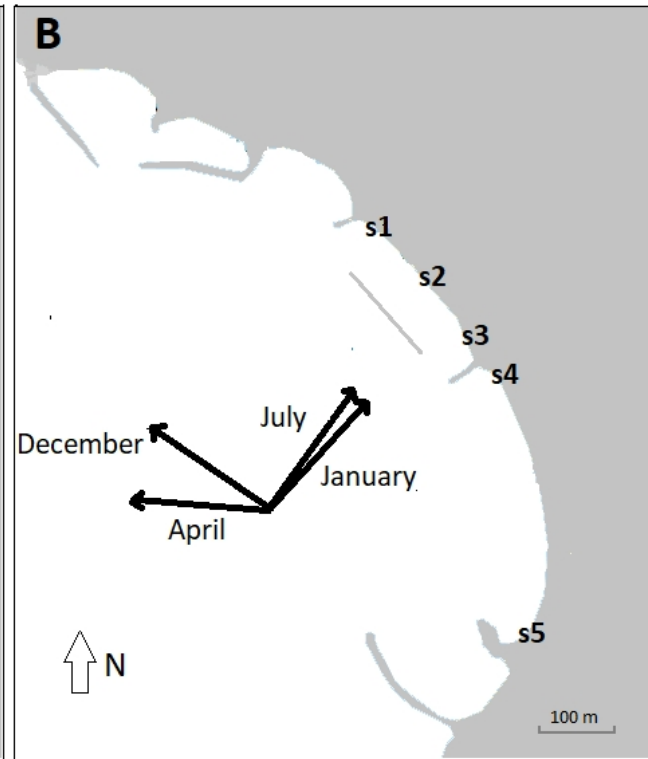
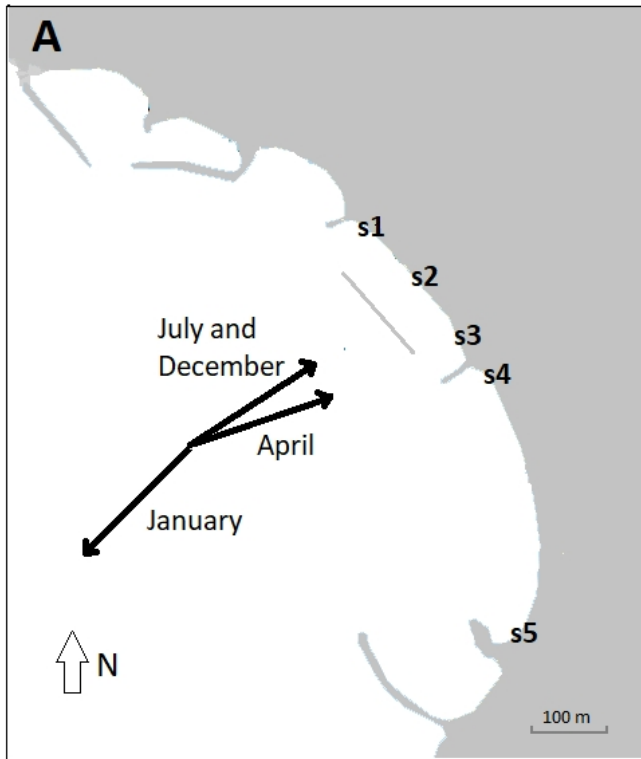
1677 Fig. 7. Plot of the RDA on fibres (A) and on fragments and spheres (B). The markers report
1678 observations (coming from the analysis of the response variables) related to single stations (Stations
1679 1-5) in the different samplings. The explanatory variables are represented by the vectors and the
1680 black squares (for the nominal variables).
1681
1682
1683
1684
1685
1686
1687
1688
1689
1690
1691
1692
1693
1694
1695
1696
1697
1698
1699
1700
1701
1702
1703
1704
1705
1706
1707
1708
1709
1710
1711

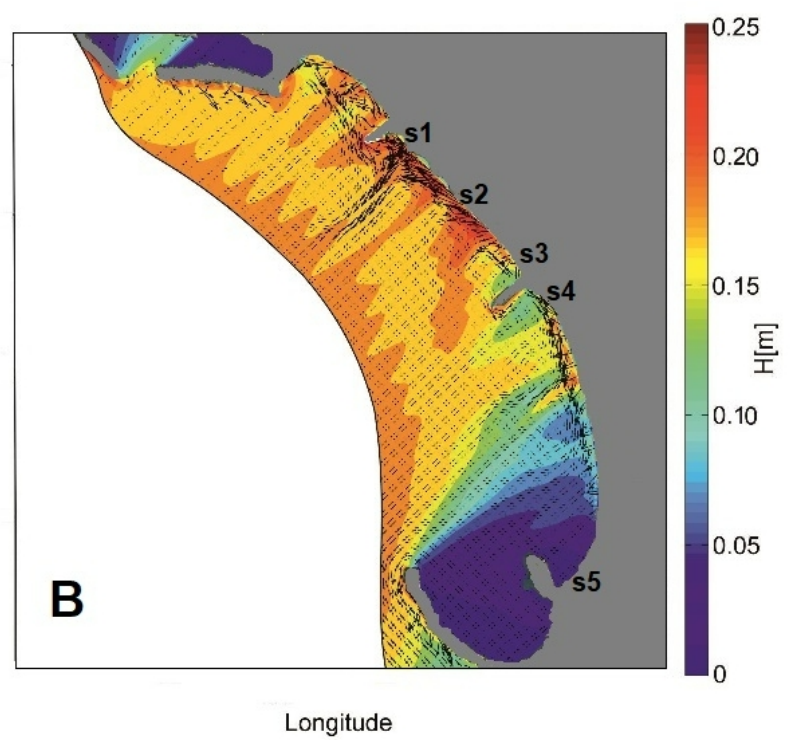
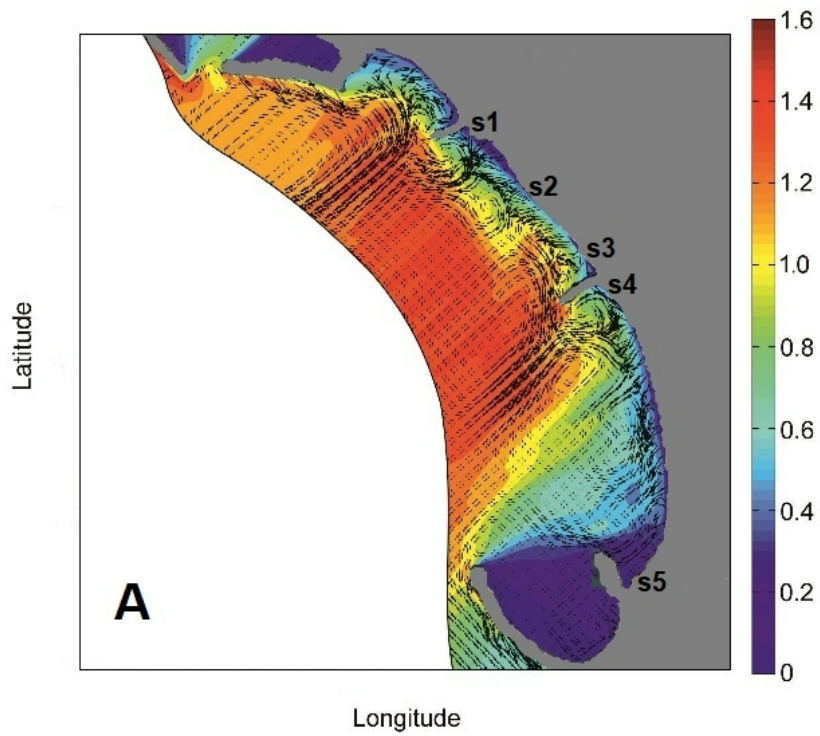












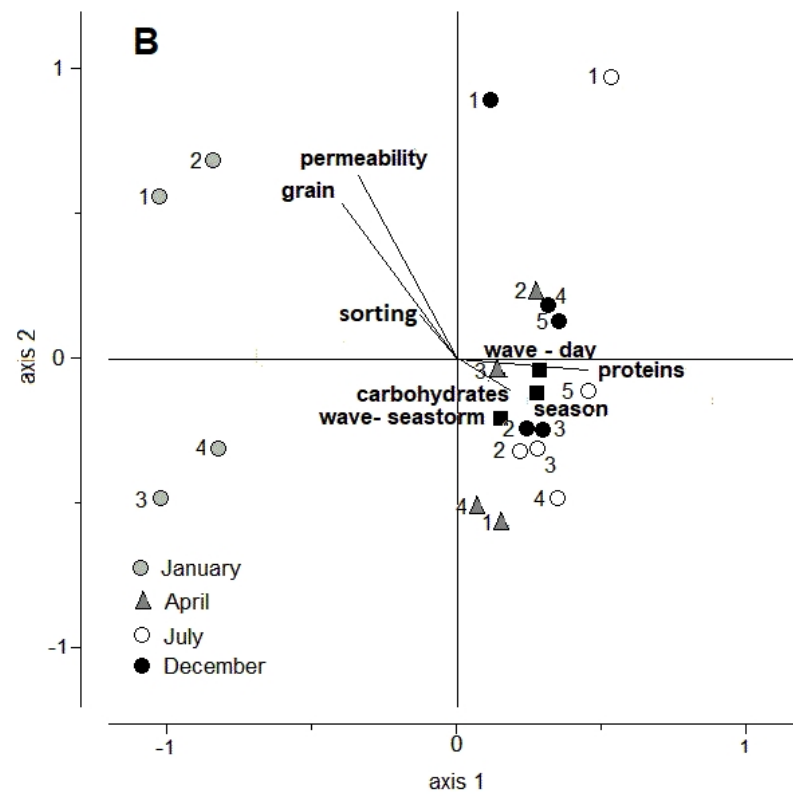
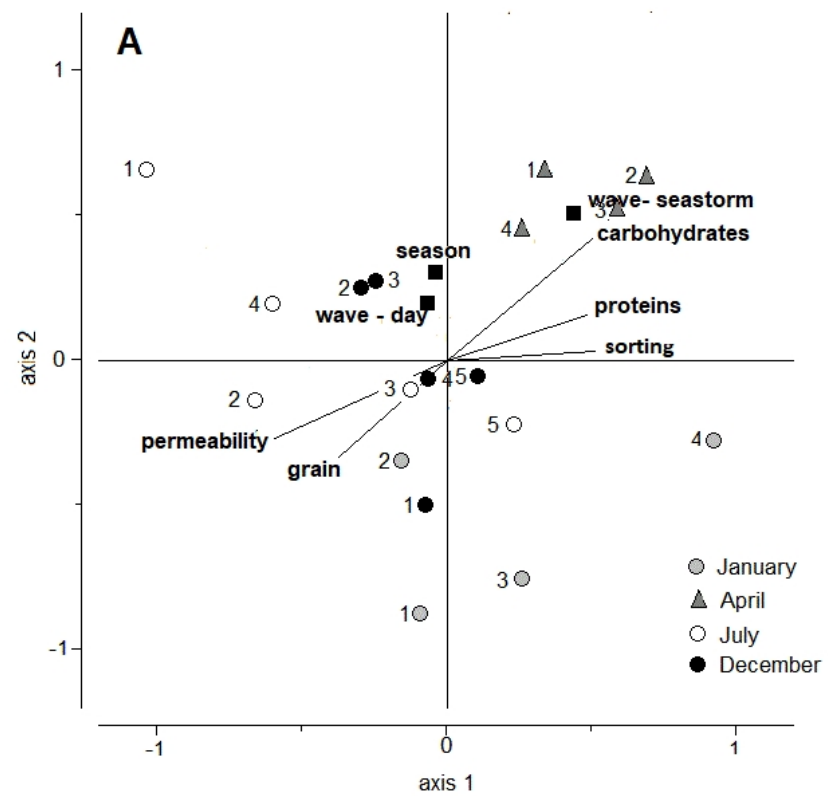


Table 1. Abundance \pm sd of fragments or spheres per kg. Na: data not available. 0: complete absence in all replicates.

	station 1		station 2		station 3		station 4		station 5	
	fragments kg ⁻¹	spheres kg ⁻¹	fragments kg ⁻¹	spheres kg ⁻¹	fragments kg ⁻¹	spheres kg ⁻¹	fragments kg ⁻¹	spheres kg ⁻¹	fragments kg ⁻¹	spheres kg ⁻¹
January	21 \pm 18	8 \pm 11	32 \pm 43	2 \pm 4	344 \pm 144	2 \pm 4	75 \pm 98	3 \pm 4	na	na
April	27 \pm 19	0	30 \pm 22	2 \pm 5	38 \pm 23	0	30 \pm 20	0	na	na
July	13 \pm 16	0	0	0	0	0	0	0	4 \pm 5	0
December	0	0	12 \pm 11	0	0	2 \pm 4	2 \pm 4	0	2 \pm 4	0

Table 2. Sediment features (mean grain size, permeability, and sorting) for each date and station.

		mean grain size		permeability		sorting	
		mm	sd	*10 ⁻² cm s ⁻¹	sd	phi	sd
17 Jan	s1	7.0	1.2	5.04	1.39	1.2	0.1
	s2	5.9	1.6	5.69	1.90	1.0	0.1
	s3	3.8	0.1	1.90	0.21	1.1	0.1
	s4	0.7	0.1	0.03	0.00	1.7	0.0
4 Apr	s1	2.1	0.4	0.52	0.06	1.2	0.2
	s2	2.1	0.5	0.17	0.02	2.0	0.3
	s3	1.5	0.1	0.12	0.01	1.6	0.1
	s4	3.6	0.2	1.08	0.19	1.2	0.1
26 Jul	s1	5.4	0.9	6.17	0.54	0.9	0.2
	s2	4.0	0.5	2.27	0.22	1.0	0.1
	s3	2.2	0.2	0.28	0.04	1.5	0.1
	s4	2.8	0.5	1.95	0.56	0.8	0.0
	s5	0.3	0.0	0.03	0.00	0.7	0.0
4 Dec	s1	5.2	2.6	1.58	2.51	2.1	0.5
	s2	1.5	0.1	0.16	0.02	1.3	0.1
	s3	0.9	0.0	0.16	0.04	1.0	0.1
	s4	1.5	0.2	0.79	0.40	0.8	0.1
	s5	0.5	0.1	0.06	0.01	0.8	0.1

Table 3. Hydrodynamic characteristics. The mean wave height (\pm sd), the significant wave height, and the direction of the waves were reported for the sampling day (only to the sampling hour), for the latest sea storm and for the other days of the week before the sampling. In January, the days of the week before the sampling are divided into two groups due to the exceptional wind event that completely changed the sea characteristics.

		mean wave height (m)	significant wave height (m)	direction ($^{\circ}$ from N)
January	sampling day	<0.1	<0.1	42-57
	storm day	2.46 \pm 0.33	2.98	216-260
	week before	1.06 \pm 0.41	2.04	144-260
	wind event	<0.1	<0.1	348-4
April	sampling day	0.20 \pm 0.02	0.24	234-294
	storm day	0.90 \pm 0.27	1.39	42-88
	week before	0.33 \pm 0.21	0.91	130-291
July	sampling day	0.85 \pm 0.07	0.91	234-240
	storm day	1.50 \pm 0.30	2.07	206-227
	week before	0.72 \pm 0.35	1.87	149-254
December	sampling day	0.30 \pm 0.05	0.40	207-247
	storm day	2.12 \pm 0.15	2.40	40-181
	week before	1.10 \pm 0.31	1.50	43-255

Table 4. RDA on abundance and colour of fibres.

axis	eigenvalue	eigenvalue as percentage of total variance	cumulative	eigenvalue as percentage of sum of all canonical eigenvalues	cumulative
1	0.285	28.5	28.5	51.3	51.3
2	0.132	13.2	41.2	23.7	74.9

Table 5. RDA on abundance and colour of fibres. The variables showing a statistically significant effect are reported in bold letters.

variable	marginal effects		conditional effects		
	eigenvalue using only one explanatory variable	eigenvalue as % (of sum all eigenvalues) using only one explanatory variable	increase total sum of eigenvalues after including new variable	F statistic	P-value
permeability	0.16	28.11	0.16	2.963	0.038
wave direction (day)	0.11	19.45	0.14	3.075	0.014
wave direction (latest seastorm)	0.15	26.74	0.14	3.351	0.016
mean grain size	0.11	19.18	0.03	0.810	0.504
proteins	0.09	16.87	0.03	0.718	0.614
season	0.05	9.79	0.02	0.515	0.756
sorting	0.07	13.44	0.02	0.346	0.860
carbohydrates	0.09	16.85	0.02	0.391	0.826

Table 6. RDA on abundance of fragments and spheres.

axis	eigenvalue	eigenvalue as percentage of total variance	cumulative	eigenvalue as percentage of sum of all canonical eigenvalues	cumulative
1	0.466	46.6	46.6	88.7	88.7
2	0.059	5.9	52.5	11.3	100.0

Table 7. RDA on abundance of fragments and spheres. The variables showing a statistically significant effect are reported in bold letters.

variable	marginal effects		conditional effects		
	eigenvalue using only one explanatory variable	eigenvalue as % (of sum all eigenvalues) using only one explanatory variable	increase total sum of eigenvalues after including new variable	F statistic	P-value
wave direction (day)	0.44	82.84	0.44	12.333	0.002
permeability	0.07	13.77	0.03	0.842	0.352
mean grain size	0.10	18.73	0.02	0.449	0.642
sorting	0.01	1.62	0.01	0.363	0.732
season	0.12	23.13	0.01	0.246	0.772
proteins	0.07	12.69	0.01	0.268	0.810
carbohydrates	0.01	2.11	0.01	0.118	0.814
wave direction (latest seastorm)	0.01	2.25	0.00	0.036	0.966

Declaration of interests

XThe authors declare that they have no known competing financial interests or personal relationships that could have appeared to influence the work reported in this paper.

The authors declare the following financial interests/personal relationships which may be considered as potential competing interests:

This research did not receive any specific grant from funding agencies in the public, commercial, or not-for-profit sectors.

Cristina Mistic, Anabella Covazzi Harriague, Marco Ferrari

Department of Earth, Environment and Life Sciences, University of Genova, Genova, Italy